Acoustic Emission based interlaminar crack growth monitoring in Carbon/Epoxy Composites

Reza Mohammadi*, Milad Saeedifar*, Mohamad Fotouhi*, Mehdi Ahmadi najafabadi[1]*, Hossein Hosseini Toudeshky**

*Non-destructive Testing Lab, Department of Mechanical Engineering, Amirkabir University of Technology, 424 Hafez Ave, 15914, Tehran, Iran.
**Department of Aerospace Engineering, Amirkabir University of Technology, Tehran, Iran

Abstract

Continuous fiber-reinforced composites, such as those consisting of carbon fibers in an epoxy resin, offer an attractive potential for reducing the weight of high-performance structures. Delamination is the most common mode of failure in these laminated composites and it leads to loss of structural strength and stiffness. In this paper, in-situ Acoustic Emission (AE) monitoring are done on the carbon/epoxy laminated composites when subjected to mode I, mode II and mixed-mode I & II loading conditions. The main objective is to investigate delamination behavior and to predict propagation curve of the delamination in different G_{II}/G_T modal ratio values by AE. First, combination of AE and mechanical data (sentry function) is used to characterize propagation stage of the delamination. Next, crack tip location during propagation of the delamination is identified using two methods. In the first method, by determining velocity of the AE waves in the specimens and some filtration methods which are applied on the AE signals, position of the crack tip is determined at any time of the tests. In the second method, cumulative energy of the AE signals is utilized for localization of the crack tip. The relationship between the cumulative AE energy and crack growth is developed and presented based on the experimental data. Agreement between the predicted crack length and actual crack length verifies the presented procedures. It can be concluded from the results that AE method is a powerful approach

[1] Corresponding author; Tel: (+98 21) 6454 3431   Fax:+98 21 8871 2838

Email address: Ahmadin@aut.ac.ir

to investigate the delamination behavior and to determine the crack tip position in the composite specimens under different loading conditions.

1. Introduction

Carbon fiber reinforced plastics (CFRP) have many advantages over other types of materials such as high specific strength, stiffness, etc. In contrary, these materials suffer from delamination defect, which is one of the most common failure mechanisms in laminated composite materials [1]. In real laminated composite structures, delamination may occur mainly in mode I, mode II or the combination of these pure modes and it will result a dramatic loss of residual strength and stiffness of the structures [2]. Therefore, there is an increasing trend to investigate this failure mechanism. Having better knowledge about the delamination failure would help to improve other parameters resulting in higher strength against crack initiation and propagation.

This paper is an attempt to investigate the initiation and propagation of delamination crack in the woven type carbon/epoxy laminated composite. To achieve this aim, Acoustic Emission (AE) technique, which has a good applicability to investigate delamination damage [3], is used. AE signal is a transient wave resulting from damage mechanisms that occur during the initiation and propagation of delamination failure. These damage mechanisms, i.e. matrix cracking, fiber failure, etc., are the origins of the AE signals that are recorded by piezoelectric transducer [4-6].

Because of low strain energy required for the delamination initiation in mode I [7], this mode is the most critical mode of delamination and there are some conducted

researches in literature regarding AE based condition monitoring of this mode [8-12]. The results of those studies have improved our understanding of mode I delamination behavior, especially in the case of damage mechanisms that occur in this mode. Although there have been some studies related to investigation of the delamination damage in the actual occurring modes, i.e. mode I, mode II and mixed mode I&II loading conditions, in composite materials by use of AE [13-16]. However, very little has been done to investigate the crack initiation and to follow the propagation of it. Since AE signals are originated from the delamination's failure mechanisms, it is possible to extract useful information about the delamination from the recorded AE data.

In this work, the aim is to enhance some applicable and sensitive AE based methods for prediction of delamination growth and behavior in the actual loading conditions (mode I, mode II and mixed-mode I&II). First, the behavior of delamination is studied using combination of the AE signals and mechanical experimental data. The method that used to combine these data is sentry function [17]. This function had acceptable results in predicting the residual torsional strength of a composite laminate after impact load, to predict the initiation stage and to evaluate the fracture toughness of the laminated composites subjected to mode I delamination [17-18]. Next, crack length during delamination of the specimens is determined by means of the recorded AE parameters. Previous studies [19-20] demonstrated the applicability of AE to localize the delamination growth in the laminated composite specimens under mode I and compression loading conditions. In this paper, to predict the delamination length, two procedures are utilized: 1) localization of the detected AE signals sources and 2)

determining a relationship between the cumulative AE energy and the length of crack. The results of sentry function and localization procedures indicate that proposed AE based methods are powerful approaches to localize the crack tip and to determine the behavior of delamination propagation in the actual loading conditions.

2. Experimental procedures

2.1. Materials and specimens preparation

The samples studied were made of 16 layers of woven carbon epoxy Prepreg. Specimens were prepared according to ASTM Standard D 5528 and D 6671 [21, 22]. The specimens were cut from CFRP panel stock with nominal dimension 175×25×4 mm^3. A 20 μm Teflon film was placed at the mid-plane to create pre-delamination. The characteristics of the specimens are represented in Table 1 and Figure 1.

Table 1 The characteristics of the specimens.

| Specimens	Specimen Name	$(\dfrac{G_{II}}{G_I + G_{II}})\%$
DCB	A	0
MMB	B_1	25
MMB	B_2	50
ENF	C	100
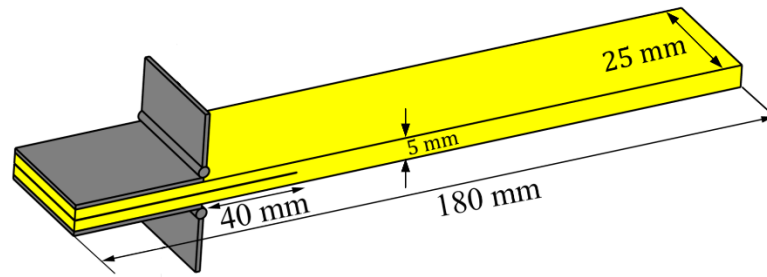
Figure 1. The dimensions of the specimens.

2.2. Test procedure

DCB, MMB and ENF test apparatus shown in Figure 2 were used to load the specimens. In DCB setup an upward force is applied to split end of the arms of specimen to create Mode I. Whereas in ENF setup, a downward load is applied to the specimen center to create Mode II. MMB is the combination of DCB and ENF. The length of the MMB lever arm can be changed to vary the G_{II}/G_T modal ratio values. In this study, G_{II}/G_T =25% and 50% modal ratio value was studied. Delamination tests were carried out at a temperature of 24°C and at a constant displacement rate of 1 mm/min. The load and displacement were continuously measured and the crack length was visually recorded using a digital camera with 25X optical zoom and 300X digital zoom.
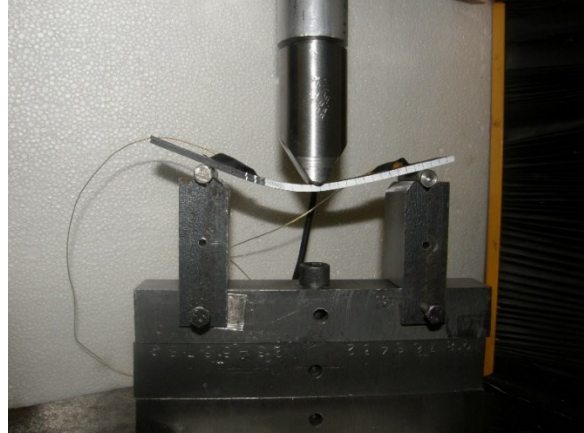
(a)   (b)
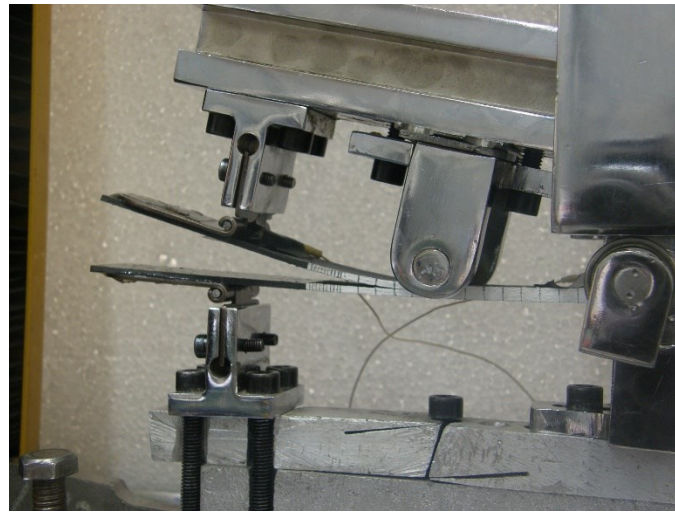
(c)

Figure 2. Test apparatus, a) DCB, b) MMB and c) ENF setups.

2.3. *Testing machine*

A properly calibrated tensile test machine (HIWA) in the range from 0.5 to 500 mm/min was used in a displacement control mode. All the specimens were loaded with constant 1 mm/min crosshead rate.

2.4. AE device

AE events were recorded by using Acoustic emission software AEWin and a data acquisition system Physical Acoustics Corporation (PAC) PCI-2 with a maximum sampling rate of 40 MHz. PICO which is a broadband, resonant-type, single-crystal piezoelectric transducer from PAC, was used as the AE sensor. The sensor has a resonance frequency of 513.28 kHz and an optimum operating range of 100–750 kHz. In order to provide good acoustic coupling between the specimen and the sensor, the surface of the sensor was covered with grease. The signal was detected by the sensor and enhanced by a 2/4/6-AST preamplifier. The gain selector of the preamplifier was set to 40 dB. The test sampling rate was 1 MHz with 16 bits of resolution between 10 and 100 dB. Prior to the damage check, the data acquisition system was calibrated for each kind of specimen, according to a pencil lead break procedure. The pencil lead break procedure enables the generation of waves at the specimen surface that are used for the device calibration. At the same time, the velocity and attenuation of the AE waves were measured. The lead breakage operation was repeated several times and at different locations between the sensors. After the calibration step, AE signals were captured during mechanical testing.

3. Results and discussion

3.1. Mechanical observation

In this work, the DCB, MMB and ENF specimens were loaded according to the procedures represented in ASTM D5528 and ASTM D6671 so as to investigate the delamination in carbon/ epoxy composites under different loading condition.

Figure 3 illustrates load-displacement and crack growth-displacement curves of the specimens. As it is obvious from Figure 3.b, the DCB specimen has stable-like crack propagation, whereas by increasing the contribution of mode II, the crack growths unstably. Thus, it is obvious that monitoring the crack growth, in mode II and mixed mode conditions with high contribution of mode II, is difficult and has some errors.

(a)   (b)
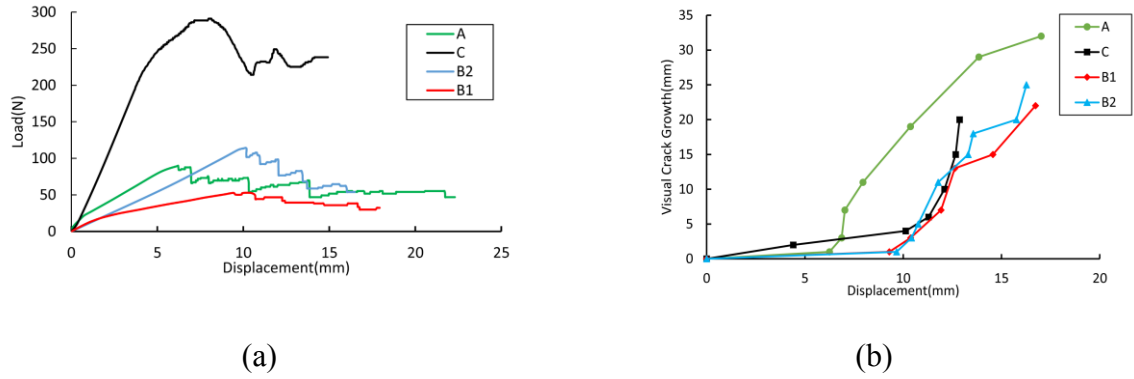
Figure 3. a) load-displacement and b) crack growth-displacement curves of the specimens.

3.2. *Sentry function*

Behavior of progression of damages in the specimen is investigated using combination of the mechanical and AE information. The function which is used for this combination is called sentry function. As indicated by Equation (1), the sentry function is stated in the logarithm form of the ratio between mechanical and acoustical energies [15]:

$$f(x) = Ln\left[\frac{E_S(x)}{E_a(x)}\right] \qquad (1)$$

Where $E_S(x)$, $Ea(x)$ and x are the strain energy, the AE events energy and the displacement, respectively. Sentry function is defined over displacement domain where the acoustic energy, $Ea(x)$, is non zero. According to progress of damages in the structure, sentry function has four trends as follow:

a) Strain energy trend (function P_1): When no damage occurs in the structure and the AE energy is negligible, by increasing the load, the mechanical energy increases and as a result the sentry function increases.

b) Sudden drop trend (function P_2): When a macroscopic damage occurs in the structure, the AE energy instantaneously increases and the sentry function drops.

c) Constant trend (function P_3): When the AE energy and mechanical energy have equilibrium state, the sentry function is constant.

d) Decreasing trend (function P_4): When the damage growth continuously, the structure degraded and sentry function has a decreasing trend.

Figure 4 shows the sentry function trends for specimens A and B_2. According to the sentry function trends, load- displacement curves could be divided into three sections. In section 1, sentry function has an increasing trend. In section 2, sharp drops could be seen in sentry function curves. In section 3, sentry function usually has a stable state. The reason for these differences is damage status in the specimen. In section 1, by increasing the load, the micro damage mechanisms such as matrix cracking occur in the specimens, but the delamination does not grow yet. In this region some small drops (P_{II} type) in the sentry function curve are observable which are related to micro damage

mechanisms, but still the material resist against the progression of macro damages and the sentry function increases. In section 2, by accumulation of the micro damages, delamination growths and AE signals with high energy appear in the specimen. Therefore, many drops occur in sentry function curve in this region. By comparing diagrams (a) and (b), it can be seen that the progression of damage in the specimen B2 with higher mode II content is more unstable than specimen A and P_{II} type functions have bigger drops compared with specimen A. In region 3, the strain energy and AE energy reaches to an equilibrium state and the sentry function has a stable state (P_{III} type).
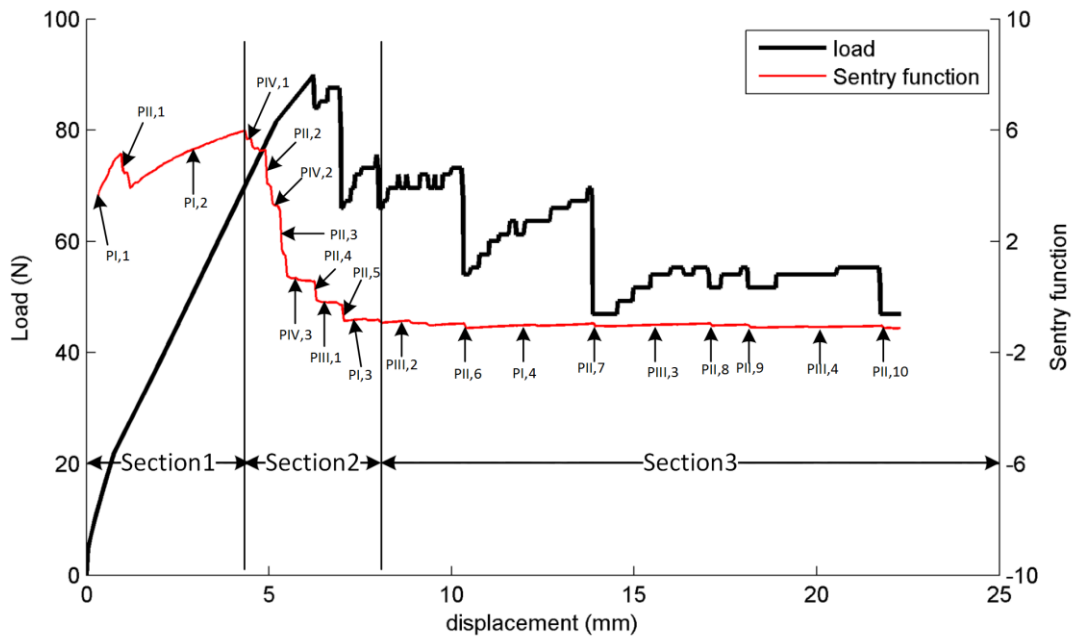
(a)
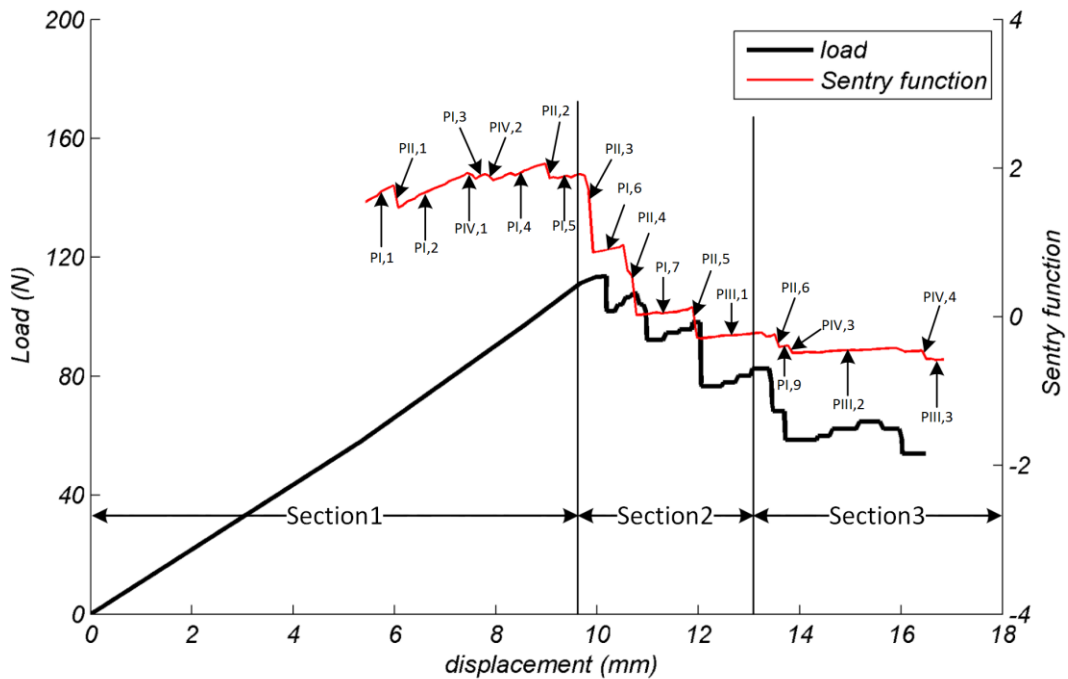
(b)

Figure 4. Sentry function trends for specimens a) A and b) B_2.

3.3. Crack Tip Localization

In this section, crack tip position in the specimens during the tests is detected using two procedures: 1) Crack tip localization using AE sources localization, and 2) Crack tip localization using cumulative AE energy.

3.3.1. Crack tip localization using determining location of the AE signal sources

AE signal is a transient wave originated by the damage mechanisms and has valuable information about the damage condition and location. In order to identify location of the AE sources in the specimens, first, velocity of the AE waves in the specimens must be determined. The velocity is calculated using standard lead breakage method. For

investigating of repeatability, the test is repeated three times for each specimen. Table 2 represents velocity of the AE wave in the specimens.

Table 2 The AE wave velocity in the specimens.

Specimen	AE wave velocity (mm/s)
A	4804306
B_1	4822077
B_2	5145330
C	4994773

Mostly, failure mechanisms, such as matrix cracking, fiber breakage and fiber/matrix debonding, occur at the small region near the crack tip during propagation of delamination. Therefore, it could be said that most of the AE signals during the tests originated from crack tip zone. As a result, by localizing the detected AE signals, it is possible to localize the crack tip. For linear localization, two AE sensors must be utilized. By employing the two sensors and post processing activities, AE noise signals that originated from out of the region between the sensors are eliminated. In this study, the first sensor is located at 15 mm before the pre-delamination tip and the second is located at 95 mm after the first sensor. As it is shown in Figure 5, when damage occurs in the specimen, the AE wave reaches to the AE sensors at different arrival times. The AE wave reaches to sensor 1 at t_1 sec and to sensor 2 at t_2 sec. By knowing arrival time differences of the AE wave to the sensors (Δt) and the AE wave velocity in the specimen (C), location of the damage can be identified according to Equation (2):

$$\begin{cases} x_1 + x_2 = 95 \\ |x_2 - x_1| = C.(t_2 - t_1) \end{cases} \; ; \; \Delta t < \frac{95}{C} \qquad\qquad (2)$$
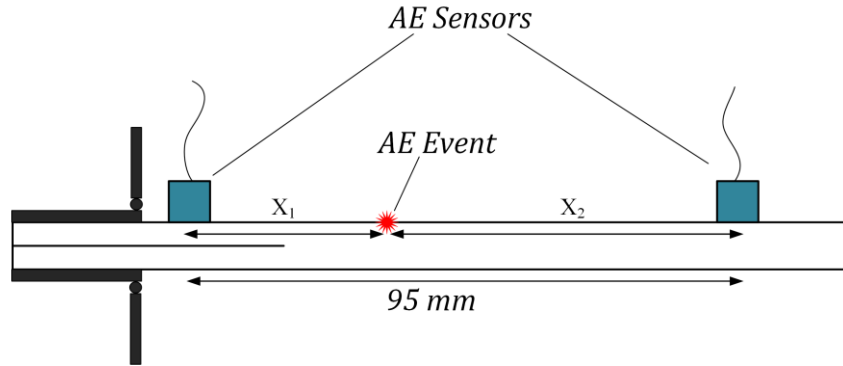

Figure 5. The AE event localization procedures.

As examples, Figure 6 shows the predicted crack tip position using the AE method versus visually-detected crack tip position for specimens A and B_1.
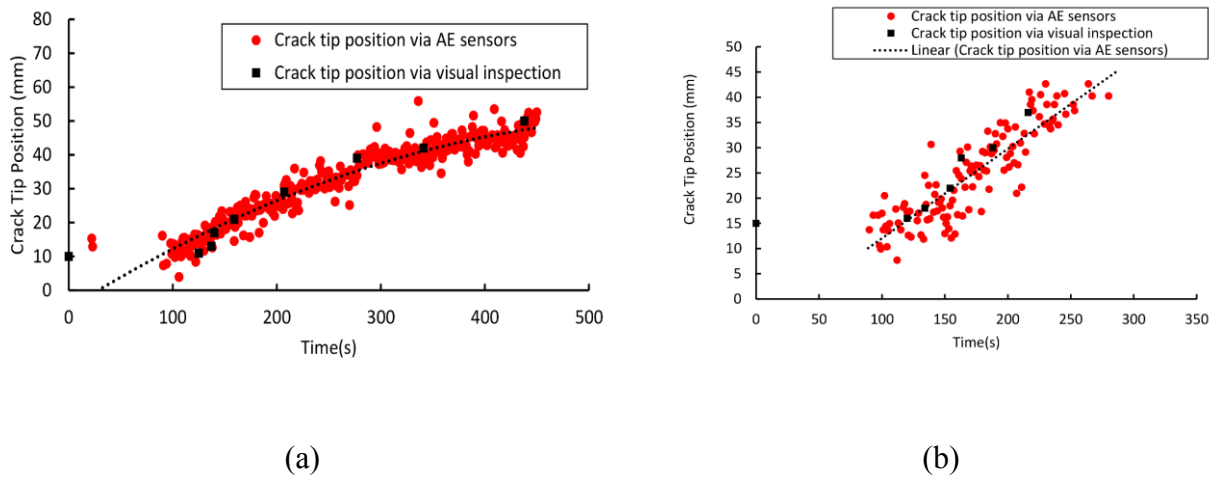

(a)

(b)

Figure 6. The predicted and actual crack tip position for specimens a) A and b) B_1.

Table 3 illustrates mean absolute differences, between the predicted values and visually detected crack tip position, for the specimens.

Table 3 The mean absolute differences of predicted values respect to actual crack tip position.

Specimen	Mean absolute errors (%)
A	17.74
B₁	6.88
B₂	10.20
C	25.51

### 3.3.2. *Crack tip localization using cumulative AE energy*

According to Figure 7, the crack growth and cumulative AE energy have a same trend with the displacement variable. As can be seen from Figure 7, each of them has a linear relation with the displacement. Thus, the crack growth can be related to the cumulative AE energy using Equation (3):

$$\left. \begin{array}{l} \Delta a = k_1 \cdot d + k_2 \\ CE = k_3 \cdot d + k_4 \end{array} \right\} \Rightarrow \Delta a = k \cdot (CE) + k_0 \qquad (3)$$

Where Δa and CE are the crack growth and cumulative energy of the AE signals, respectively. k_1, k_2, k_3, k_4, k and k_0 are coefficients of the equations that are related to the material properties and loading conditions.
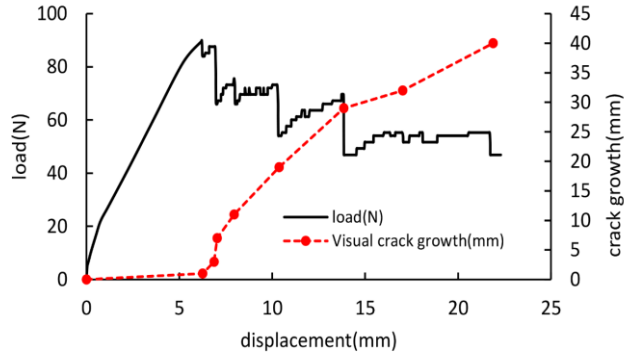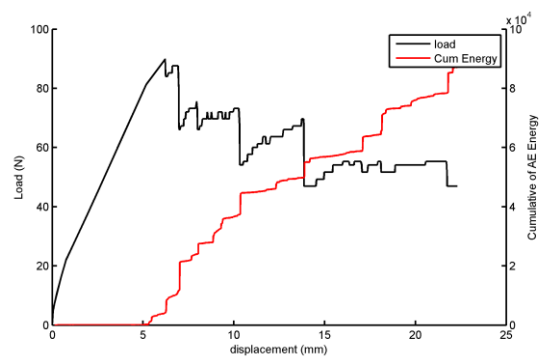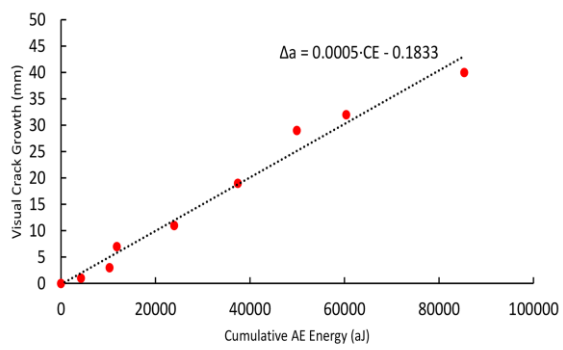
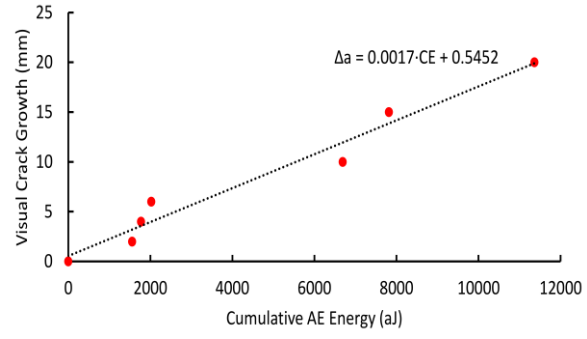(a)   (b)

Figure 7. a) Crack growth and b) Cumulative AE energy curves for specimen A.

Figure 8 shows linear relation between the crack growth and cumulative energy for specimens A and C.
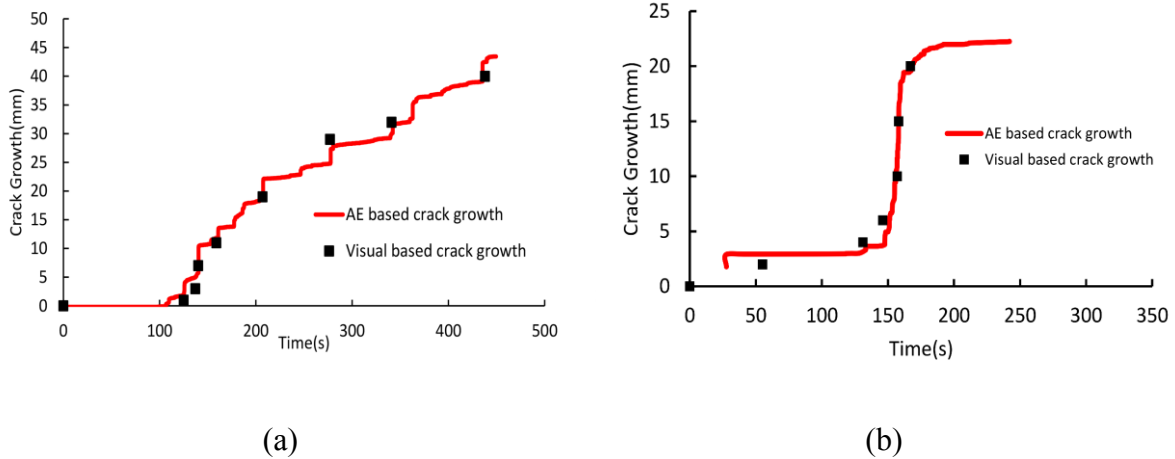

(a)   (b)

Figure 8. The linear relation between crack growth and cumulative energy for specimens a) A and b) C.

Figure 9 shows the predicted crack growth vs. the visual crack growth curves for specimens A and C. As the results show, this method could predict the crack growth very well.

(a)   (b)

Figure 9. Predicted crack growth vs. visual crack growth curves for specimens a) A and b) C.

Table 4 illustrates mean absolute differences, between the predicted values with the visually detected crack tip position, for the specimens. The results obtained from the cumulative AE energy method is more accurate than the AE localization method to predict the crack length. Advantage of the cumulative AE energy method is that it could be done just by one AE sensor. In addition, in this procedure, location of the sensor on the specimens is not important and there is no need to determine the AE wave velocity in the specimens.

Table 4 The mean absolute differences between the predicted and actual crack tip position.

Specimen	Mean absolute errors (%)
A	5.10
B_1	0.8
B_2	1.45
C	5.61

4. Conclusion

In this study, AE was used to monitor delamination behavior of the carbon/epoxy laminated composites, under mode I (DCB), mode II (ENF) and mixed-mode I & II (MMB) loading conditions. Then, the AE and mechanical results were utilized to investigate propagation behavior of the delamination. The results showed that the delamination growth has unstable behavior under mode II and mixed mode near mode II loading condition and visual detection of the crack tip is difficult in these modes. Two developed AE-based methods were proposed to localize the crack tip during delamination growth. In the first method, by determination AE wave velocity in the specimens and linear localization method, the crack tip position was determined. In the second method, using relation between the crack growth and cumulative AE energy, the crack tip position was predicted. The investigation shows that AE leads to the results which are in excellent agreement with the visually detected results and can solve the weaknesses, especially in mode II and mixed-mode conditions where unstable crack growth and difficult crack monitoring during propagation exist.

5. Acknowledgment

6. References

1. Sridharan S. Delamination Behaviour of Composites, CRC Press 2008, New York.

2. Pagano NJ and Schoeppner GA. Delamination of polymer matrix composites: Problems and Assessment. In: Kelly A, Zweben C, editor. Comprehensive Composite Materials. Elsevier Science, 2000; 433-528.

3. Bohse J and Brunner AJ. Acoustic emission in delamination investigation. In: Sridharan S. Delamination behaviour of composites. CRC Press, New York, 2008; 217–277.

4. Godin N, Huguet S and Gaertner R. Integration of the Kohonen's Self-Organizing Map and k-Means Algorithm for the Segmentation of the AE Data Collected During Tensile Tests on Cross-Ply Composites. NDT&E Int 2005; 38(4): 299–309.

5. Huguet S, Godin N, Gaertner R, Salmon L and Villard D. Use of acoustic emission to identify damage modes in glass fibre reinforced polyester. Compos Sci Technol 2002; 62(10–11):1433–1444.

6. Fotouhi M, Heidary H and Ahmadi M. Characterization of composite materials damage under quasi-static 3-point bending test using Wavelet and Fuzzy C-Means Clustering. J Compos Mater 2012; 46(15): 1795–1808.

7. Pereiraa AB and de Morais AB. Mode I interlaminar fracture of carbon/epoxy multidirectional laminates. Compos Sci Technol 2004; 64:2261–2270.

8. Barre S and Benzeggagh ML. On the use of acoustic emission to investigate damage mechanisms in glass-fiber reinforced polypropylene. Compos Sci Technol 1994; 52:369–376.

9. Bohse J, Krietsch T, Chen JH and Brunner AJ. Acoustic emission analysis and micro-mechanical interpretation of mode I fracture toughness tests on composite materials. European Structural Integrity Society 2000; 27: 15-26.

10. Sause MGR, Müller T, Horoschenkoff A and Horn S. Quantification of failure mechanisms in mode-I loading of fiber reinforced plastics utilizing acoustic emission analysis. Compos Sci Technol 2012; 72 (2): 167-174.

11. Pashmforoush F, Fotouhi M and Ahmadi M. Acoustic emission-based damage classification of glass/polyester composites using harmony search k-means algorithm. J Reinf Plast Compos 2012; 31 (10): 671-680.

12. Fotouhi M and Ahmadi Najafabadi M. Acoustic emission-based study to characterize the initiation of delamination in composite materials. J Thermoplast Compos Mater 2014; DOI: 0892705713519811.

13. Benzeggagh ML and Kenane M. measurement of mixed-mode delamination fracture toughness of unidirectional glass/epoxy composites with with mixed-mode bending apparatus. Compos Sci Technol 1996; 56: 439-449.

14. Benmedakhene S, Kenane M and Benzeggagh MD. Initiation and growth of delamination in glass/epoxy composites subjected to static and dynamic loading by acoustic emission monitoring. Compos Sci Technol 1999; 59: 201–208.

15. Fotouhi M and Ahmadi Najafabadi M. Investigation of the mixed-mode delamination in polymer-matrix composites using acoustic emission technique. J Reinf Plast Compos 2014; 33 (19): 1767-1782.

16. Saeedifar M, Fotouhi M, Ahmadi Najafabadi M and Hosseini Toudeshky H. Interlaminar Fracture Toughness Evaluation in Glass/Epoxy Composites Using

Acoustic Emission and Finite Element Methods. J Mater Eng Perform 2014; DOI: 10.1007/s11665-014-1291-2.

17. Refahi Oskouei A, Zucchelli A, Ahmadi M, et al. An integrated approach based on acoustic emission and mechanical information to evaluate the delamination fracture toughness at mode I in composite laminate. Mater Des 2011; 32: 1444–1455.

18. Minak G and Zucchelli A. Damage evaluation and residual strength prediction of CFRP laminates by means of acoustic emission techniques, In: Durand LP, editor. Composite Materials Research Progress, Nova Science Publishers Inc, New York, 2008; 165–207.

19. Romhany G and Szebényi G. Interlaminar fatigue crack growth behavior of MWCNT/carbon fiber reinforced hybrid composites monitored via newly developed acoustic emission method. eXPRESS Polym Lett 2012; 6(7): 572-580.

20. Paget CA. Delamination Location and Size by Modified Acoustic Emission on Cross-ply CFRP Laminates during Compression-Compression Fatigue Loading. ICCM17 proceedings 2009; UK.

21. ASTM D5528–01. Standard Test Method for Mode I Interlaminar Fracture Toughness of Unidirectional Fiber-Reinforced Polymer Matrix Composites. ASTM International, West Conshohocken, PA, 2007.

22. ASTM D 6671/D 6671M − 03. Standard Test Method for Mixed Mode I-Mode II Interlaminar Fracture Toughness of Unidirectional Fiber Reinforced Polymer Matrix Composites. ASTM International, West Conshohocken, PA, 2004.

List of captions

List of Figure captions:

Figure 1. The dimensions of the specimens.

Figure 2. Test apparatus, a) DCB, b) MMB and c) ENF setups.

Figure 3. a) load-displacement and b) crack growth-displacement curves of the specimens.

Figure 4. Sentry function trends for specimens a) A and b) B_2.

Figure 5. The AE event localization procedures.

Figure 6. The predicted and actual crack tip position for specimens a) A and b) B_1.

Figure 7. a) Crack growth and b) Cumulative AE energy curves for specimen A.

Figure 8. The linear relation between crack growth and cumulative energy for specimens a) A and b) C.

Figure 9. Predicted crack growth vs. visual crack growth curves for specimens a) A and b) C.

List of table captions:

Table 1. The characteristics of the specimens.

Table 2. The AE wave velocity in the specimens.

Table 3. The mean absolute errors between predicted and actual crack tip position.

Table 4. The mean absolute errors between predicted and actual crack tip position.